ASSESSMENT OF MULTIANGULAR POLARIZATION CONTRIBUTION TO THE BIDIRECTIONAL REFLECTANCE OF NATURAL SAMPLES

Georgi T. Georgiev[a], James J. Butler[b], Kurt J. Thome[b], K.Jon Ranson[b], Michael D. King[c]

[a] Sigma Space Corp., Lanham, MD 20706, e-mail: georgi.t.georgiev@nasa.gov
[b] NASA Goddard Space Flight Center, Greenbelt, MD 20771
[c] University of Colorado, Boulder, CO 80309

ABSTRACT

Assessment of the effect of multiangular polarized incident light on the bidirectional reflectance factor (BRF) of vegetation and soil samples is presented in this paper. The samples were evaluated with a reference to 99% white Spectralon calibration standard in the UV-VIS-NIR spectral range. The BRF of the samples was found to be strongly influenced by the polarization of the incident light at different multiangular geometries.

Index Terms— BRF, Reflectance, Multiangular, Polarization, Remote Sensing

1. INTRODUCTION

Although there are a number of studies on polarized reflectance from vegetation [1], soil and snow [2], natural surfaces [3], etc. little attention has been devoted to the case of a polarized source and an unpolarized detector, an instrument architecture that is common to many space-borne instruments deploying lasers as sources. An excellent study of Spectralon polarization properties illuminated by coherent light was published by Haner et al. [4] Spectralon panels were quantified in terms of their Bidirectional Reflectance Distribution Function (BRDF), which was measured at laser wavelengths of 442.0, 632.8, and 859.9 nm. In-plane BRDF data was presented with reference to the polarization states of the source and detector.

The current study expands our previous work on the BRF dependence on the polarization of the incident light of Spectralon [5] to vegetation [6] and regolith samples. A regolith sample was obtained from a validation site in Etosha Pan, Namibia. The vegetation leaves are from the black locust tree (Robinia pseudoacacia).

2. MEASUREMENTS

The BRF measurements were performed on NASA's Goddard Space Flight Center Diffuser Calibration Laboratory's Scatterometer [7]. The BRDF is defined in radiometric terms as reflected surface radiance in a given direction divided by the incident surface irradiance from another direction. The incident irradiance is the radiant flux incident on the surface. The reflected surface radiance is the light flux reflected through solid angle Ω per projected solid angle [8]:

$$BRDF = \frac{L_s(\theta_i, \phi_i, \theta_s, \phi_s, \lambda)}{E_i(\theta_i, \phi_i, \lambda)} = \frac{P_s / \Omega}{P_i \cos\theta_s} \qquad (1)$$

where P_r is the reflected radiant power, Ω is the solid angle determined by the area of detector aperture, A, and the radius from the sample to the detector, R. The solid angle can be computed as $\Omega = A/R2$. P_i is the incident radiant power, and θ_r is the reflected zenith angle.

We deal with BRF (R_λ) here as it is better used by the remote sensing community. The R_λ is expressed following van de Hulst [9] formulation:

$$R_\lambda(\theta, \theta_0, \Phi) = \frac{\pi I_\lambda(\theta, \theta_0, \Phi)}{\mu_0 F_\lambda}, \qquad (2)$$

where I_λ is the measured reflected intensity (radiance), F_λ is the solar flux density (irradiance) incident on the top of the atmosphere, θ and θ_0 are respectively the viewing and incident zenith angles, Φ is the azimuthal angle between the viewing and incident light directions, and $\mu_0 = \cos\theta_0$. The bidirectional reflectance factor (BRF) is dimensionless and numerically equivalent to the product of BRDF and π.

A xenon lamp/monochromator tunable assembly with a well-defined incoherent illumination was used at 340nm, 470 nm, and 870 nm. All the samples, including vegetation, soil and Spectralon were illuminated with parallel (P) and perpendicular (S) linearly polarized light at incidence angles of 0^0, 45^0, 60^0 and 67^0, scatter zenith angles from 0^o to 80^o, and scatter azimuth angles of 0^o and 180^o. The BRF of natural samples, i.e. vegetation and soil, was measured at wavelengths of 340, 470 and 870nm, whereas the Spectralon was measured at 300nm, 350nm, 400nm, 500nm, 600nm, 700nm, 800nm and 900nm. Both the natural samples and Spectralon were also measured at 0^o, and 45^o incident angles while changing the polarization of the linearly polarized incident light from S to P by rotating the polarizer in 10 degree steps.

3. RESULTS AND DISCUSSIONS

For comparison purposes in this study, the quantity, BRF(p-s), is defined as the percent difference of the BRF measured with P polarized incident light (BRFp) and the BRF measured with S polarized incident light (BRFs) divided by the BRF using unpolarized incident light. In the discussion which follows, the difference is computed using Eq. 3:

$$BRF(p-s) = \left[{}^{(BRFp - BRFs)}/_{BRF}\right] x\ 100 \qquad (3)$$

The dependence of Spectralon on the polarization of the incident light is presented in Fig.1 at angle of incidence (AOI) of 0^o, although 45^o and 60^o incident angles were also tested. The in-plane BRF(p-s) at P or S polarized incident light shows small spectral dependence from 300nm to 900nm, consistent with the well-known spectral reflectance of Spectralon at these wavelengths. The difference increases with increasing scatter zenith angle and is as large as 5% at normal incidence and 80^o scatter zenith. The reflection of the P polarized incident light decreases with increasing scatter zenith angle until the pseudo-Brewster angle is reached and then increases beyond that angle but the reflection of the S polarized incident light increases at a faster rate.

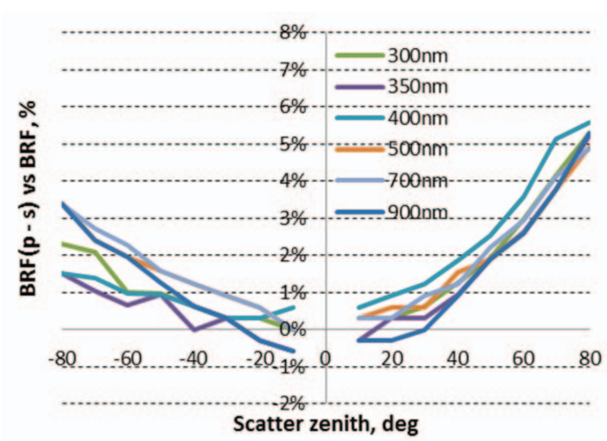

Fig.1: Spectralon polarization dependence at normal incidence

The in-plane BRF(p-s) of fresh green leaves from the black locust tree at normal incidence is shown in Fig.2 for 340nm, 470nm and 870nm although the BRF(p-s) at 870nm is negligible and follows the shape of the Spectralon case. This is due to the scattering at this wavelength being predominantly a bulk scattering phenomena within the leaf rather than a surface scatter. The BRF(p-s) at 340 nm and 470 nm differs significantly from the Spectralon case. It depends strongly on the scatter zenith angle and is as high as 38% at 80^o scatter zenith.

The BRF dependence on the polarization of the incident light is attributed to the electronic transition of pigments to the excited singlet state, and whether the dipoles are oriented parallel or perpendicular to the oscillating electric vector of the incident polarized light. The light will then be preferentially absorbed when incident light polarization and dipoles are aligned, thus reducing the reflection from the specimen. The effect of incident light polarization on BRF is greatest at in-plane and out-of-plane geometries that coincide with P or S polarization of the incident light. In turn, the BRF(p-s) is smaller when the scatter azimuth angle is 45^o from the P and/or S polarization of the incident light due to the orientation of the dipoles.

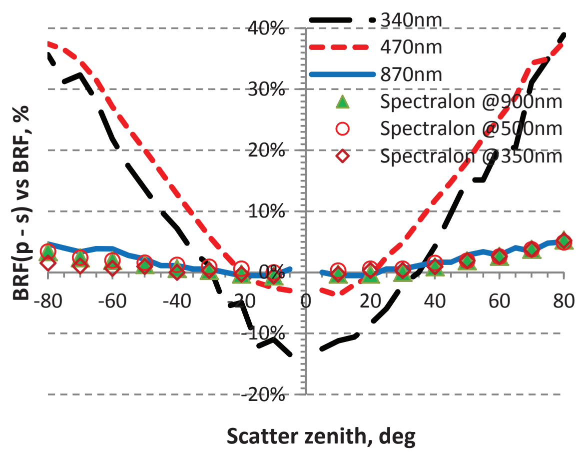

Fig.2: Polarization dependence of leaves at normal incidence

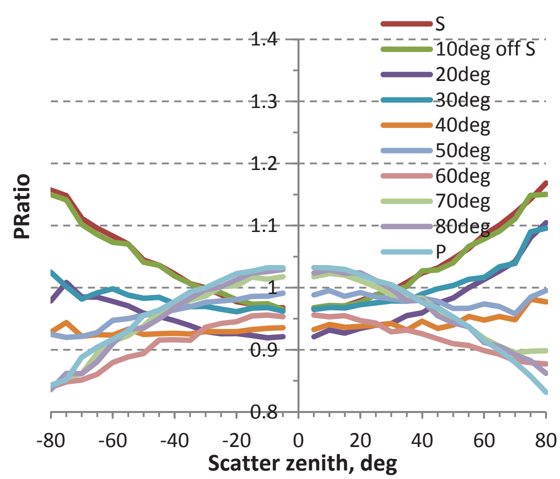

Fig.3: PRatio at AOI = 0deg, 470nm, vegetation, black locust

The BRF of the black locust tree leaves was also studied when the polarization of the incident light changed from S polarization to P polarization by rotating the Scatterometer incident light polarizer in steps of 10^o. The BRF at a specific polarization of the incident light is presented as a ratio between the BRF measured at the specific polarization and the BRF at unpolarized incident light, called the PRatio and shown in Eq.3 below. These measurements were performed at normal and 45^o incident angles. The results are shown in Fig.3 for AOI = 0^o and Fig.4 for AOI = 45^o. The BRF depends strongly on the orientation of the linear polarization of the incident light on the sample. At AOI = 0^o the PRatio increases/decreases at larger scatter zenith angles and the difference is higher at the pure P and S polarizations. At AOI = 45^o the PRatio at large scatter zenith angles clearly shows the effect of the incident light polarization in forward direction. The PRatio at scatter zenith angles less than 5^o shows independence of the polarization of the incident light from the scatter zenith angle.

$$PRatio = {}^{BRF_{pol}}\!\big/_{BRF_{unpol}} \tag{3}$$

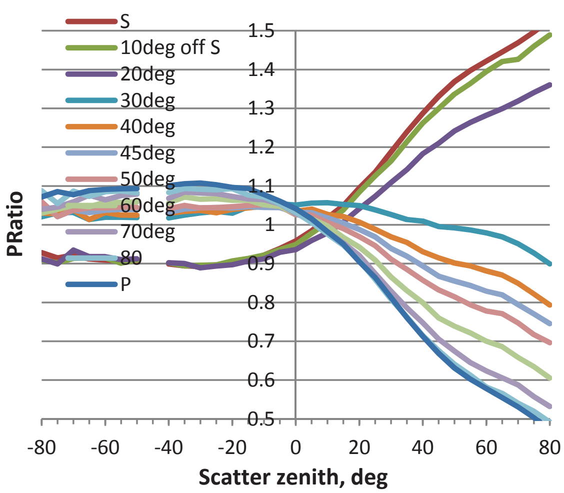

Fig.4: PRatio at AOI = 45deg, 470nm, vegetation, black locust

The three Etosha Pan regolith samples, which are different fraction sizes (Fr) of the same material, were defined as follows: Fr.1<0.5mm, 0.5mm<Fr.2<1mm and 1mm<Fr.3<2mm. The BRDF of these samples at 340, 470, and 870nm are presented in Fig. 5 at AOI = 0^o. The regolith has close to Lambertian reflectance for unpolarized incident light however for polarized incident light, the regolith reflectance behaves differently than the Spectralon due to its high mineral content, which is dominated by four compounds, (i) feldspar and mica, (ii) feldspar and sepiolite, (iii) silicates, and (iv) calcite and dolomite. The reflectance from these compounds is polarization sensitive thus determines the samples' reflectance spectra. The BRF(p-s) of all three regolith samples do not present any significant difference based on their fraction size or wavelength both at normal and 45^o incident angle, therefore only the 470nm case is plotted in Fig.6. The Spectralon's BRF(p-s) at 500nm is included as a reference. The polarization dependence of the regolith decreases with increasing scatter zenith angle, an opposite trend compared to that of the Spectralon.

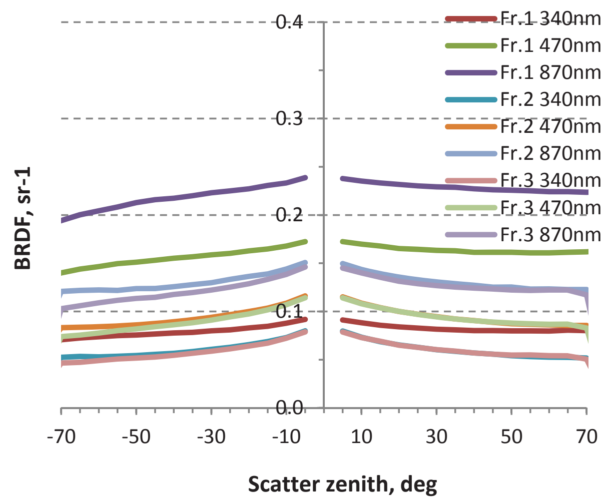

Fig.5: BRF of three regolith fractions

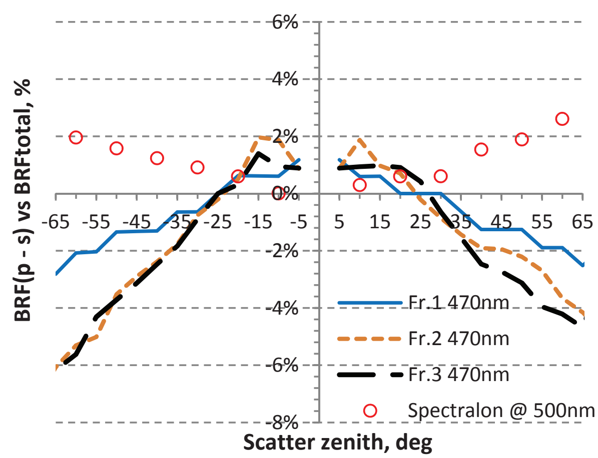

Fig.6: Polarization dependence of regolith at normal incidence

The impact of polarization on the regolith's BRF when the polarization of the incident light was changed from S polarized to P polarized by positioning the polarizer at 0^o

(S), 20°, 45°, 70° and 90° (P) is shown in Fig.7 for AOI = 0° and Fig.8 for AOI = 45°. The PRatio is very close but not equal to 1.00 at 45° polarizer positioning, increasing toward S polarization and decreasing toward P polarization at AOI = 0°. At AOI = 45° the PRatio is independent of the polarization of the incident light from the scatter zenith angle at scatter zenith angles less than 5°.

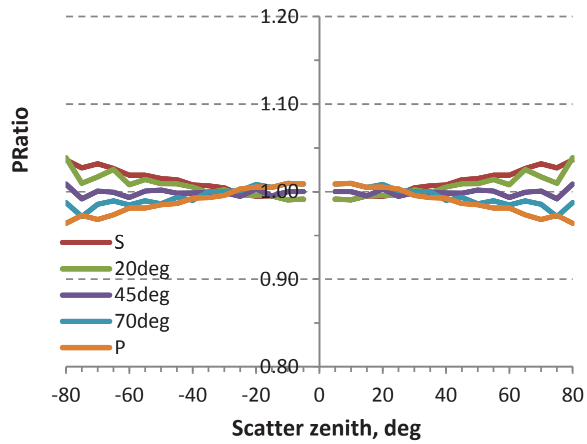

Fig.7: PRatio at AOI = 0deg, regolith Fr.2

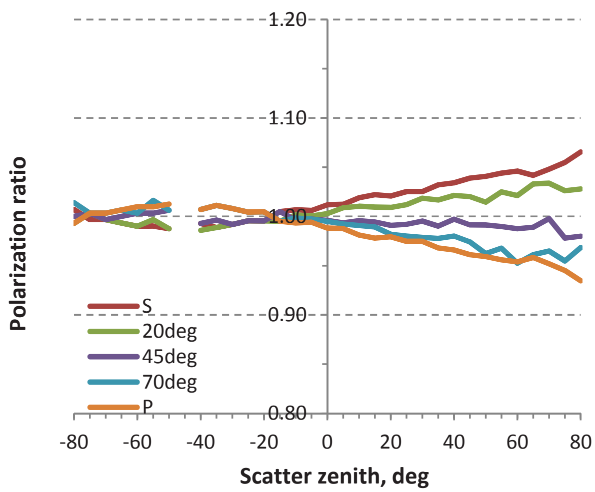

Fig.8: PRatio at AOI = 45deg, regolith Fr.2

4. CONCLUSIONS AND FUTURE WORK

The laboratory results indicate that the often overlooked impact of polarization effects in the reflectance of vegetation and soils may need to be considered as the requirements on accuracy of remote sensing data continue to become more stringent. The results from studies such as the one presented here will be of interest to the remote sensing community both in developing sensor design requirements and in providing constraints for modeling and correction efforts of airborne and satellite-based data. The results of this study are primarily important in comparing remote sensing data acquired with active (polarized source) and passive (unpolarized source) instruments. For instance, the different behavior in the BRF(p-s) for vegetated material relative to soils as shown in Figures 2 and 6 may be useful in differentiating these materials from space. While such differentiation is currently feasible through multispectral analysis, it is not as feasible for active sensors relying on single wavelengths. The use of the PRatio may provide a method for differentiating between soils and vegetation, though based on the data shown here, it would require viewing scattering angles beyond the backscatter case. The results from this work also indicate what portion of the reflected light comes from the surface of the vegetation and what portion is from leaves subsurface scattering giving insight into the plant physiology.

6. REFERENCES

[1] L. Grant, "Diffuse and specular characteristics of leaf reflectance", *Remote Sens. Environ.*, vol.22, pp.309-322, 1987,

[2] J. Peltoniemi, T. Hakala, J. Suomalainene, E. Puttonen, "Polarized bidirectional reflectance factor measurements from soil, stones and snow", *J. of Quantitative Spectroscopy and Radiative Transfer*, vol.110, pp.1940-1953, 2009,

[3] F. Maignan, F-M. Bréon, E. Fédèle, M. Bouvier, "Polarized reflectances of natural surfaces: Spaceborne measurements and analytical modeling", *Remote Sens. Environ.*, vol.113, pp.2642-2650, 2009,

[4] D.A. Haner, B.T. McGuckin, C.J. Bruegge, "Polarization characteristics of Spectralon illuminated by coherent light", Appl. Optics, vol. 38, no.30, pp.6350-6356, 1999.

[5] G.T. Georgiev**,** J.J. Butler, "The effect of incident light polarization on Spectralon BRDF measurements", *Proc. SPIE Sensors, Systems, and Next-Generation Satellites VIII.*, vol.5570, pp.492-502, 2004,

[6] G.T. Georgiev, J.J. Butler, K.J. Thome, K.J. Ranson, M.D. King: "The effect of incident light polarization on vegetation bidirectional reflectance factor", IGARSS '10, pp.1652-1655, Jul.25-30, 2010

[7] G.T. Georgiev, J.J. Butler, "Long-term calibration monitoring of Spectralon diffusers BRDF in the air-ultraviolet", *Applied Optics*, 2007, vol.46, No.32, pp.7892-7899

[8] F.E. Nicodemus, J.C. Richmond, J.J. Hsia, I.W. Ginsburg, T. Limperis, "Geometrical Considerations and Nomenclature for Reflectance," National Bureau of Standards, NBS Monograph 160, 1977,

[9] H.C. van de Hulst, *Multiple light scattering, Tables, Formulas, and Applications*, vol. 1, San Diego: Academic Press, 1980.